

RELATIONSHIP BETWEEN THE PACIFIC OCEAN SST
VARIABILITY AND THE GANGES-BRAHMAPUTRA RIVER
DISCHARGE

A Thesis
Presented to
The Academic Faculty

By

Jun Jian

In Partial Fulfillment
Of the Requirements for the Degree
Master of Science in School of
Earth and Atmospheric Sciences

Georgia Institute of Technology
May 2005

RELATIONSHIP BETWEEN THE PACIFIC OCEAN SST
VARIABILITY AND THE GANGES-BRAHMAPUTRA RIVER
DISCHARGE

Approved by:

Dr. Webster, Peter , Advisor
School of Earth and Atmospheric Sciences
Georgia Institute of Technology

Dr. Black, Robert
School of Earth and Atmospheric Sciences
Georgia Institute of Technology

Dr. Wang, Yuhang
School of Earth and Atmospheric Sciences
Georgia Institute of Technology

Date Approved: Marth 31st, 2005

ACKNOWLEDGEMENTS

This thesis is a much cooperative work and many people shared their suggestions and experiences with me. Foremost is my advisor Dr. Peter J. Webster, whose instruction was invaluable. As my thesis reading committee member, Prof. Yuhang Wang and Prof. Robert X. Black went over the draft carefully and provided many good suggestions.

My officemates Carlos Hoyos and Violeta Toma provided helpful suggestions and a good environment. Other colleagues, Dr. Dan Collins, Dr. Chang Hai-Ru and Dr. Claire Cosgrove have shared my presentations in our group meeting and their constructive questions helped me too.

My wife took every effort in daily life to help me get this paper completed. And my parents encouraged me as well. Without all these people's help I could not get my work done. Their compassion, kindness and patience I will keep in my mind forever.

TABLE OF CONTENTS

ACKNOWLEDGEMENTS	iii
LIST OF TABLES	v
LIST OF FIGURES	vi
SUMMARY	viii
CHAPTER 1 INTRODUCTION	1
1.1 Description of Ganges-Brahmaputra- Meghna River System	1
1.2 History of Forecasting River Flows by SST	5
1.3 El Niño/Southern Oscillation (ENSO) phenomena	6
1.4 Indian monsoon Introduction	11
1.5 Previous research on the precipitation and outflow from Ganges catchment	17
CHAPTER 2 DESCRIPTION OF DATASETS	20
CHAPTER 3 RESULTS AND DISCUSSIONS	22
3.1 Relationship between Brahmaputra discharge and SST	22
3.1.1 Seasonal relationship	22
3.1.2 June Brahmaputra discharge and northwestern Pacific SST	25
3.2 Relationship between Ganges discharge and SST	28
3.2.1 Boreal summer discharge and SST	28
3.2.2 Monthly discharge with monthly SSTs	30
3.3 Verification results by other analysis methods	34
3.3.1 Outliers detection by scatter plots	34
3.3.2 Significance study by composite analysis	36
3.3.3 Summer river discharge in different ENSO periods	38
3.4 The SST evolution relative to southwest Pacific SST	40
CHAPTER 4 CONCLUSIONS AND FUTURE EXPECTATION	43
REFERENCES	44

LIST OF TABLES

Table 1.1	Bangladesh droughts, floods and cyclones, 1960-1992	4
-----------	---	---

LIST OF FIGURES

Figure 1.1	The catchment's area of Brahmaputra-Ganges-Meghna Rivers	2
Figure 1.2	Schematic diagram of normal, El Niño, and La Niña condition in the Pacific Ocean	8
Figure 1.3	Seasonal (Jun-Jul-Aug) Climate anomalies during El Niño (La Niña) conditions	10
Figure 1.4	Monsoon areas	11
Figure 1.5	Simplified sketch of thermal monsoon circulation	13
Figure 1.6	Surface winds in northern hemisphere during summer and winter	15
Figure 2.1	Time series of Brahmaputra-Ganges River discharge over period 1990-2000	21
Figure 3.1	Correlation map of seasonal (Jul-Aug-Sep) Brahmaputra discharge with seasonal SST and compared with 1998's data removal	24
Figure 3.2	Relation map of June Brahmaputra discharge and lead time northwest Pacific SST over period 1956-2003	26
Figure 3.3	Scatter points of June Brahmaputra discharge verses northwest Pacific Ocean SST index	27
Figure 3.4	Correlation map of seasonal (Jul-Aug-Sep) Ganges discharge with seasonal SST	29
Figure 3.5	Correlation map of July and August Ganges discharge with monthly SST	31
Figure 3.6	Lagged correlations between two river discharges of seasonal SST and monthly SST	33
Figure 3.7	Scatter points of Nino3.4 SST and southwest Pacific SST verses July Ganges discharge data	35
Figure 3.8	Composite analysis of Ganges and Brahmaputra discharge relative to ENSO over a 50 year period	37

Figure 3.9	JJAS discharge categorized by ENSO and magnitude	39
Figure 3.10	Correlation map of May southwestern Pacific SST with leading time SSTs	42
Figure 3.11	Correlation map of May southwestern Pacific SST index with lag time SSTs	42

SUMMARY

A simple correlation analysis was used to investigate the linear relationships between sea surface temperature (SST) and monthly flow of Ganges and Brahmaputra at the borders of Bangladesh and India using approximately 50 years of river discharge data. Strong correlations were found between the equatorial Pacific SST and boreal summer Ganges discharge from three-month lag to two-month lead times. The El Niño-Southern Oscillation (ENSO) explains Ganges flow variance exceeding 0.95 significance level using both the Nino 3.4 SST correlation and the composites made for El Niño (La Nina) periods.

The May SST of the southwest Pacific Ocean to the east of Australia continent has a strong correlation (>0.6) with early summer Ganges discharges. Using a lag correlation analysis of Ganges discharge and SST, we found a steady and continuous development in the Nino 3.4 SST relationship, and a strong correlation with the southwest Pacific SST which is most pronounced three-four months prior to the onset of Asian summer monsoon. These relationships mean that at least 25% of the interannual summer Ganges River discharge variability can be explained by antecedent equatorial and southwest Pacific SST. It provides a possible statistical method for linear forecasting two or three months in advance.

The Brahmaputra River discharge, on the other hand, shows weak relationships with tropical SST variability except for the Bay of Bengal and the higher northern latitudes of the Pacific.

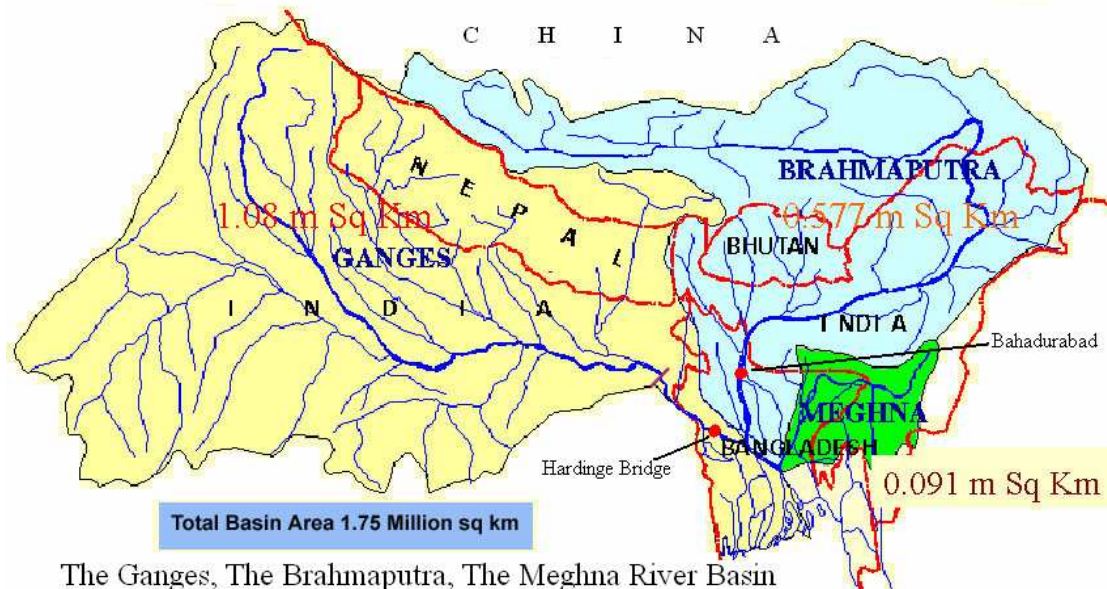
CHAPTER 1

INTRODUCTION

1.1 Description of Ganges-Brahmaputra-Meghna River System

Bangladesh occupies an area of about 145,000km² between latitudes 20.5°N and 26.75°N, and longitudes 88°E and 92.75°E. It is bounded on the west, north and east by India, on the Southeast corner by Myanmar, and on the south by the Bay of Bengal. The Bangladesh delta is fed by two of the largest river systems in the world: the Brahmaputra and Ganges, which extend across the great plains of northern India and the Assam region, respectively, plus smaller catchments in the east such as the Meghna (Figure 1.1).

About 20 percent of the country is regularly inundated by flood waters which are considered benign as they maintain soil fertility, floodplain fish lands and bio-diversity (COMET-IT 2004). Even severe periodic flooding is common. Since 1954, flooding has covered 37 percent of the land once every 10 years such as in the summer of 1998 when over 60% of Bangladesh was in flood for nearly three months.



The Ganges, The Brahmaputra, The Meghna River Basin

Figure 1.1 The catchment's area of Brahmaputra-Ganges-Meghna rivers system (SDNP 2004), Bangladesh, India, China and Nepal along the principal channels of the rivers

Extensive floods greatly affect the marginal population. These people lose whatever assets they have and suffer from water related disease, loss of work and wage. People who live in perennially flooded zones generally have low levels of health, nutrition and education.

Reports indicate that there is little evidence of significant negative effects on annual agricultural production levels though millions of acres of cropland are regularly flooded and crops are washed away. In fact, major floods are typically followed by bumper harvests. This may be due to extensive distributions of nutrients from the flooding, higher water tables, and the efforts taken by disaster mitigation

programs such as Agricultural Rehabilitation Program. This program provides aid to significantly increase production for the next crop season.

While this may be true, there are also field reports indicating that the quality of water is rapidly declining. Also the silt carrying floods, which were once considered a soil fertilizer, are now carrying excessive amounts of sands which now cover entire fields making them useless for cultivation. This is true for the tri-river basin as well as for the peninsular region.

Flash floods cause serious damage to crops, property fish stock and other resources particularly in the north, north-east and eastern part of the country. Each year, less dramatic floods and droughts also occur throughout the summer but with sufficient irregularity to cause significant societal consequences and disruptions to agricultural activities. The affected areas and losses by disasters such as droughts, floods and hurricanes during the period of 1961 to 1992 are displayed in Table 1.1.

Table 1.1 Bangladesh droughts, floods and cyclones, 1960-1992 (Ericksen et al. 1997)

Date	(% area of country)	Flood (area affected 000 sq.km)	% of the Country	Cyclone (storm surge in metres)	Crop Damage (000s Mt)	Deaths Reported
1960				4.5-6 (09 Oct)		3,000
1960				2.5-3 (30Oct)		5,149
1960	2.7	28.4	19.13			
1961	22.4	28.8	19.40			
1961				6-9 (09 May)		11,466
1962	11.3	37.2	25.06			
1963	8.6	43.1	29.04			
1963				4-5 (28 May)		11,520
1964		31.0	20.89			
1964				- (11 April)		196
1965		28.4	19.13			
1965				3.5 (11 May)		19,279
1965				4.5-6 (14Dec)		873
1966	18.4	33.4	22.50			
1966				4.5-9 (10 Oct)		850
1967		26.7	17.99			
1968		37.2	25.06			
1969		41.4	27.89			
1969				- (17 Apr)		75
1970	9.1	42.4	28.57			
1970				- (23 Oct)		300
1970				6-9(12 Nov)		220-400,000
1971	4.8	36.3	24.46			
1972	42.9	20.8	14.01			
1973		29.8	20.08			
1973				1.5-7.5(O9Dec)		183
1974		52.6	35.44			28,000
1974				2-5(28 Nov)		a few
1975		16.6	11.18			
1976	5.1	28.3	19.07			
1977		12.5	8.42			
1978	3.7	10.8	7.20			
1979	42.1					
1980		33.0	22.23			
1981		3.14	2.16	2 (10Dec)		2
1982	N.A.					
1983	N.A.	11.1	7.48		321	
1984		28.2	19.00		1257	
1985		11.4	7.68	3-4.5(25 May)	59	11,069
1986		4.6	3.09		140	
1987		57.3	38.61		1327	1,700
1988		89.97	60.62		2110	1,600
1988				1.5-3(29 Nov)	575	2,000
1989		6.10	4.11			
1990		3.5	2.35			
1991		28.60	19.27	6-7.5 (29 Apr)		138,868
1992		2.0	1.35			

Another 18 damaging cyclones affecting Bangladesh did not result in reported deaths, making a total of 35 cyclones in 32 years.

1.2 History of Forecasting River Flows by SST

The forecasting of river flow has been an important goal for scientists and engineers for centuries. Nowhere has the need been more urgent in the Bangladesh delta. Given the societal impact of floods in the tropics, it is surprising how few fundamental studies have been undertaken to develop schemes for their prediction. Those that do exist have concentrated on seasonal prediction. For example, Amarasekera et al. (1997) attempted to relate interannual SST variability with discharge for a wide-range of tropical and subtropical rivers. They found that the Amazon and Congo discharges were essentially uncorrelated with Pacific SST variability. On the other hand, higher correlations were found between subtropical rivers such as the Nile and the Parana and with El Niño-Southern Oscillation. The Nile appears to be the most extensively studied river basin with the development of a number of predictive schemes (e.g., Wang et al. 1999, Tawfik 2003, Eldaw et al. 2003) all of which show similar relationships as Amarasekera et al. (1997). However few studies have concentrated on the Ganges-Brahmaputra system. The Bangladesh prediction problem is especially acute because no upstream data is available to Bangladeshi technicians and engineers, and, the Ganges and Brahmaputra must be considered as un-gauged river basin.

1.3 El Niño-Southern Oscillation (ENSO) phenomena

El Niño is a disruption of the ocean-atmosphere system in the tropical Pacific having important consequences for weather and climate around the globe. In normal, non-El Niño conditions (upper panel of Figure 1.2), the trade winds blow towards the west across the tropical Pacific. These winds pile up warm surface water in the west Pacific, so that the sea surface is about half meter higher at Indonesia than at Ecuador. The SST is about 8°C higher in the west, with cool temperatures off South America, due to an upwelling of cold water from deeper levels. Rainfall is found in rising air over the warmest water, and the east Pacific is relatively dry. (NOAA 2004a, b)

During El Niño conditions (middle panel of Figure 1.2), the trade winds relax in the central and western Pacific leading to a depression of the thermocline in the eastern Pacific, and an elevation of the thermocline in the west. The result was a rise in SST and a drastic decline in primary productivity. Rainfall follows the warm water eastward, with associated flooding in Peru and drought in west Pacific: Indonesia and Australia. The eastward displacement of the atmospheric heat source overlaying the warmest water results in large changes in the global atmospheric circulation, which in turn force changes in weather in regions far removed from the tropical Pacific.

La Niña condition (bottom panel) is nearly the opposite of El Niño: the trade winds get enhanced associated with unusually cold SST in the eastern equatorial

Pacific, thermocline is depressed in western Pacific and elevated in east. It is much wetter than normal across the Pacific Northwest and dryer and warmer across much of the southern tier. The two phenomena often follow each other resulting in a cycle with a period of 2-7 years.

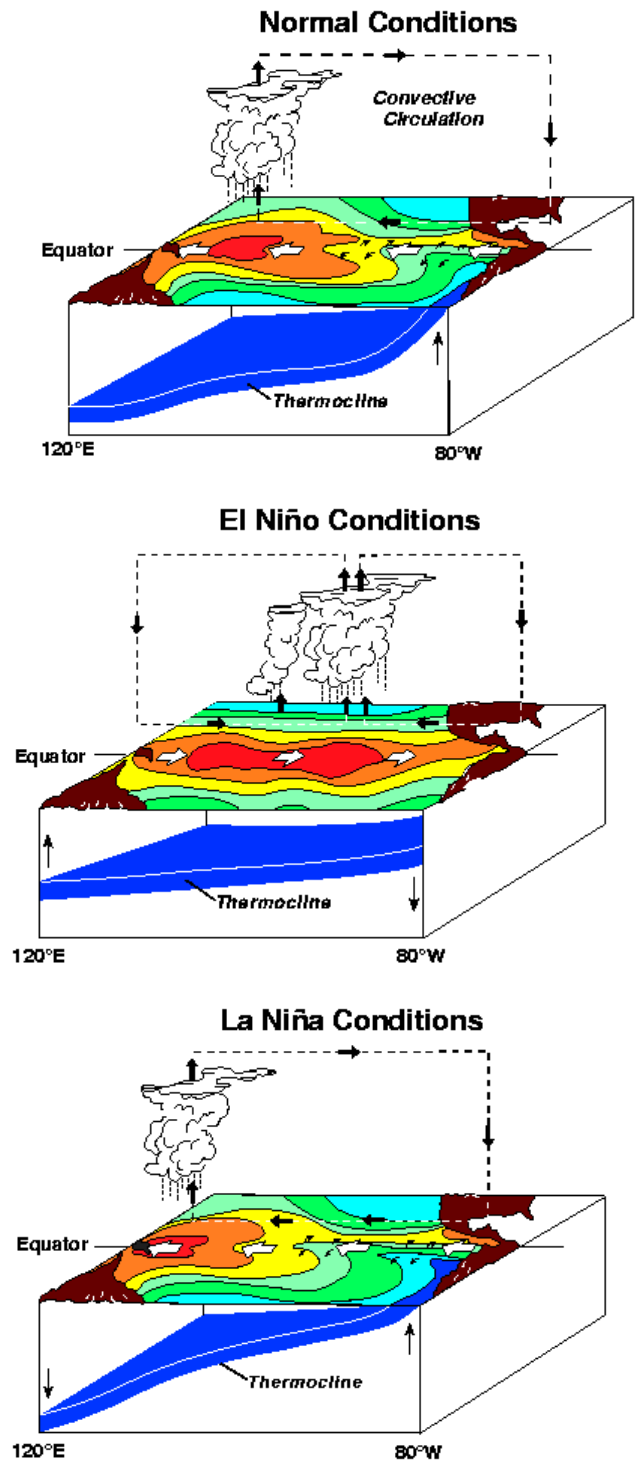


Figure 1.2 Schematic diagram of normal, El Niño, and La Niña conditions in the Pacific Ocean (NOAA 2004c)

The Southern Oscillation Index (SOI) represents the sea level pressure (SLP) difference between the Darwin, Australia and Tahiti which is observed to be strongly correlated with equatorial Pacific Ocean SST variations. In general, the Southern Oscillation refers to the atmospheric component of the El Niño- Southern Oscillation (ENSO) system. There has been extensive research on ENSO in recent decades. A good description of ENSO can be found in Encyclopedia of Atmospheric Sciences (Nicholls, 2003).

The regional climate consequences of El Niño and La Niña phenomena are shown in Figure 1.3. It appears reasonable that the most affected regions are around the tropical Pacific Ocean considering the extreme SST anomalies that occur in the central equatorial Pacific. Among these regions the South Asian continent, known as a monsoon dominated area, is the furthest west. During warm episodes (El Niño), it is relatively dry on the Indian sub-continent and anomalously wet and cool during La Niña episodes. However, most of the Ganges River catchments fall into this area.

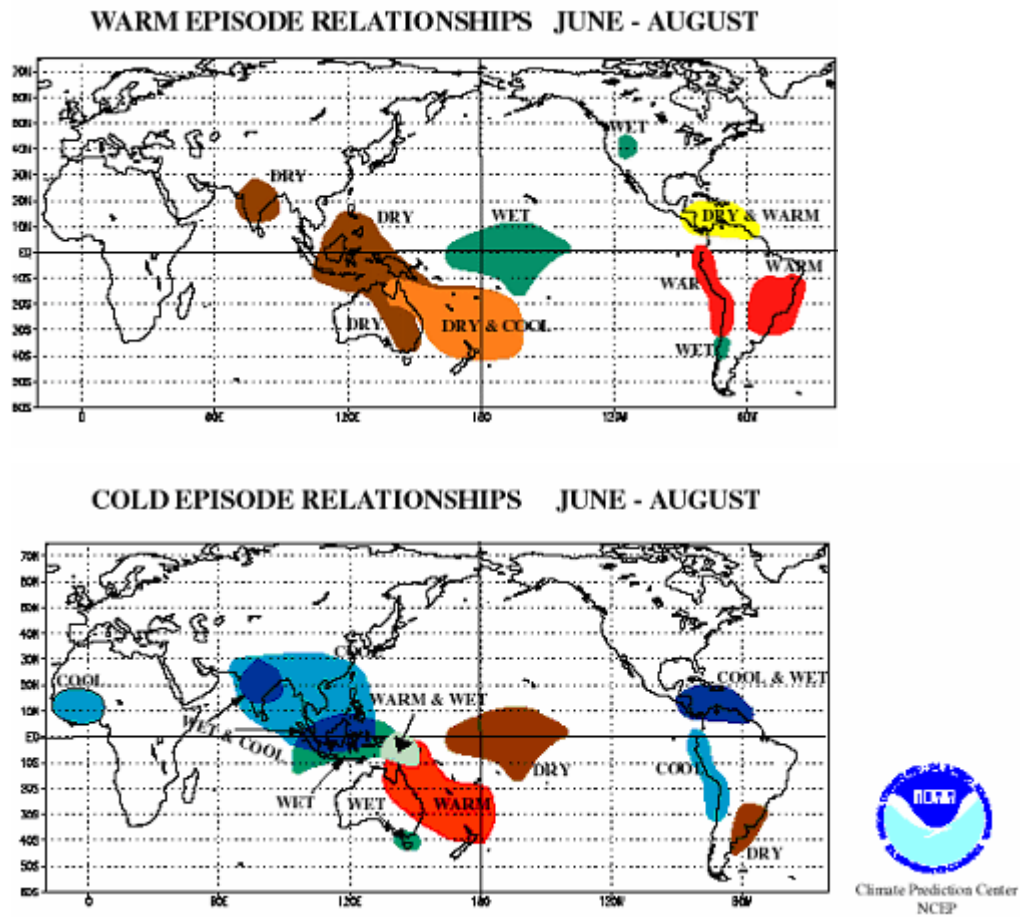


Figure 1.3 Seasonal (Jun-Jul-Aug) Climate anomalies during El Niño (La Niña) conditions (NCEP/ CPC 2004)

1.4 Introduction of Indian monsoon (Joint Agricultural Weather Facility, 2004)

“A monsoon is defined as a seasonal shift in wind direction, being derived from the Arabic word “mausim”, meaning season.” Generally it is based on a wind speed at least 3 meters per second. In the place heavily influenced by monsoon, seasonal wind reverses its direction and causes a drastic change on precipitation and temperature. The monsoon related phenomenon is the dominant feature of low-latitude climates stretching from West Africa to the western Pacific Ocean (Figure 1.4).

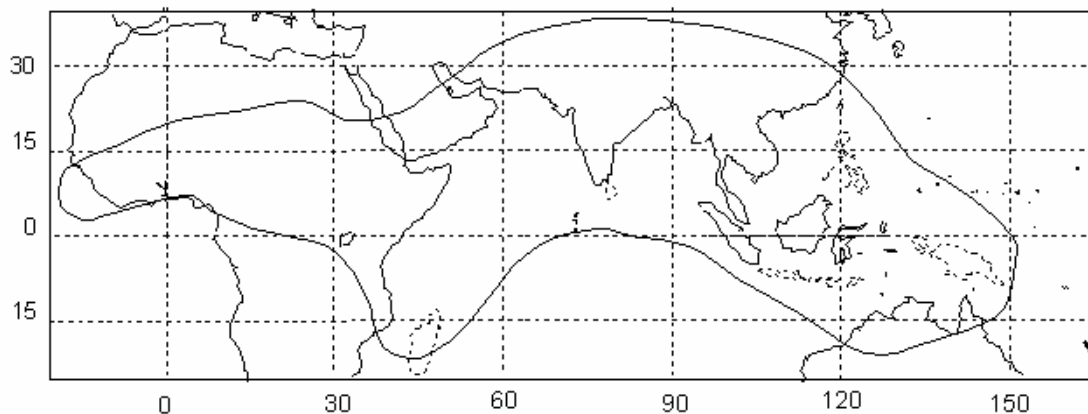


Figure 1.4 Monsoon areas enclosed by solid line (Oliver and Fairbridge, 1987)

For hundreds of years, the monsoon has been observed by sailors and was used for wind-driven ships. The systematic study of the seasonal and interannual variations of the mean monsoon patterns began in the late 19th century with the incentive to predict the Indian rainfall after the great drought in 1877. Sir Gilbert Walker (1923, 1924, 1928) figured out that the global climate possesses a coherent low-frequency variability. As Webster (1987, 1998) has noted in his monsoon reviews, it has been

recognized for hundreds of years that the physics behind the annual monsoon cycle is the variation of incoming solar radiation and the differential heating rate of the surface of land and water. Sections of the earth's surface heat and cool at different rates depending on their ability to absorb incoming solar radiation and the magnitude of this incoming shortwave radiation. Water's heat capacity is much larger than soil and rock, which allows it to store energy more efficiently than the land surface and therefore retain heat longer. During summer the land heats more rapidly than the adjacent ocean because of its smaller specific heat and shallow layer depth. In the winter the land surface will cool much more quickly than the ocean simply because there is little available heat in the subsurface that can be made available to heat the surface on seasonal time scales (Webster et al. 2003). To maintain atmospheric energy balance, heat is generally transferred from areas of surplus to deficit, and in the case of a land-water differential, this is accomplished through a phenomenon known as the "land-sea breeze". On a larger scale when there is a land-water contrast, such as a continent surrounded by oceans, heat build up on land over summer time will warm air masses, lower their density, increase their vertical volumes, and drive up the height of pressure levels. Thus, in the same height of the upper troposphere, the pressure is higher over continent than ocean. This build-up pressure gradient between the land and ocean will drive air masses move from land to ocean in the upper troposphere. As a result of this convection, the air masses in the vertical column get much greater over the ocean than land. Denser air associated with high pressure dominates ocean surfaces. Surface air will blow from ocean to land resulting in a pressure gradient and

also construct the summer monsoon circulation. The winter monsoon circulation comes from the similar mechanism but result in a conversely direction (Figure 1.5). Air converging into a low pressure center at the surface rises, leading to moisture condensation and the subsequent release of heat into the upper atmosphere. Diverging air at the surface in a high pressure center is associated with subsiding air from the upper atmosphere and evaporation, a mechanism for energy storage.

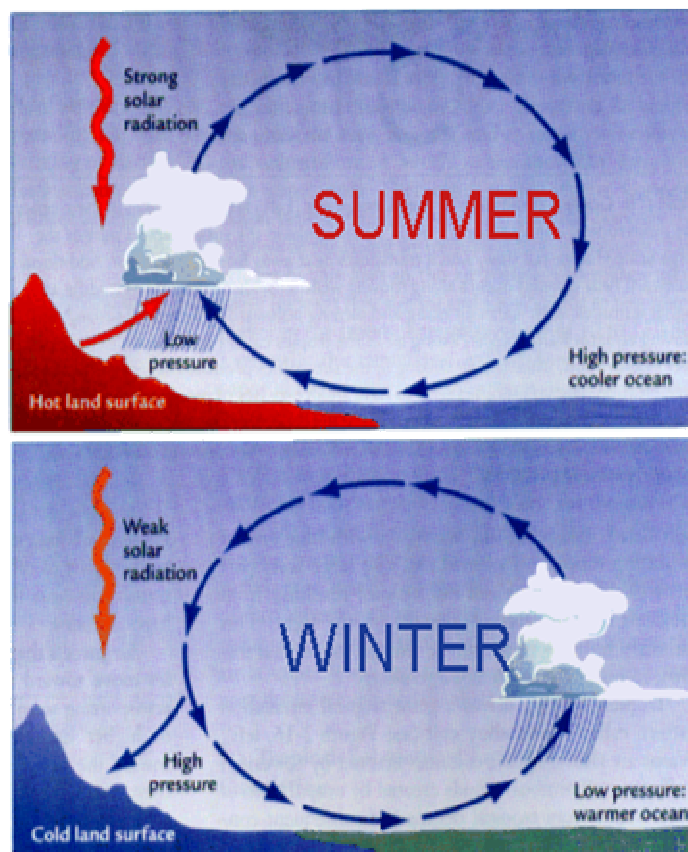


Figure 1.5 Simplified sketch of thermal monsoon circulation (from website)

Just as energy imbalances develop between land and water surfaces, seasonal and latitudinal variations in temperature are driven primarily by variations of insolation

and average solar zenith angle. The hemisphere in the boreal summer has lower average zenith angle due to the earth's tilt and therefore receives the most direct radiation and experiences a net radiative heating (more energy is gained than lost). The winter hemisphere is at the same time experiencing net radiative cooling. For compensation, heat is transported from warmer to cooler areas by ocean and wind currents. Since the areas of heat surplus and deficit change throughout the year, the direction of transport must change as well. Figure 1.6 shows low latitude surface wind directions averaged over the summer and winter seasons. Note that winds change their directions after crossing the equator because of the Coriolis force. Climates dominated by monsoons experience the most pronounced seasonal wind direction shifts. In the South Asian, the rainy season, typically beginning in June, is preceded by nearly two months of scorching temperatures, cooled only with the commencement of the summer rains brought on by the southwesterlies from the Indian Ocean. January is the peak of the dry season, which is marked by cool, dry northeasterly flow over most of the region.

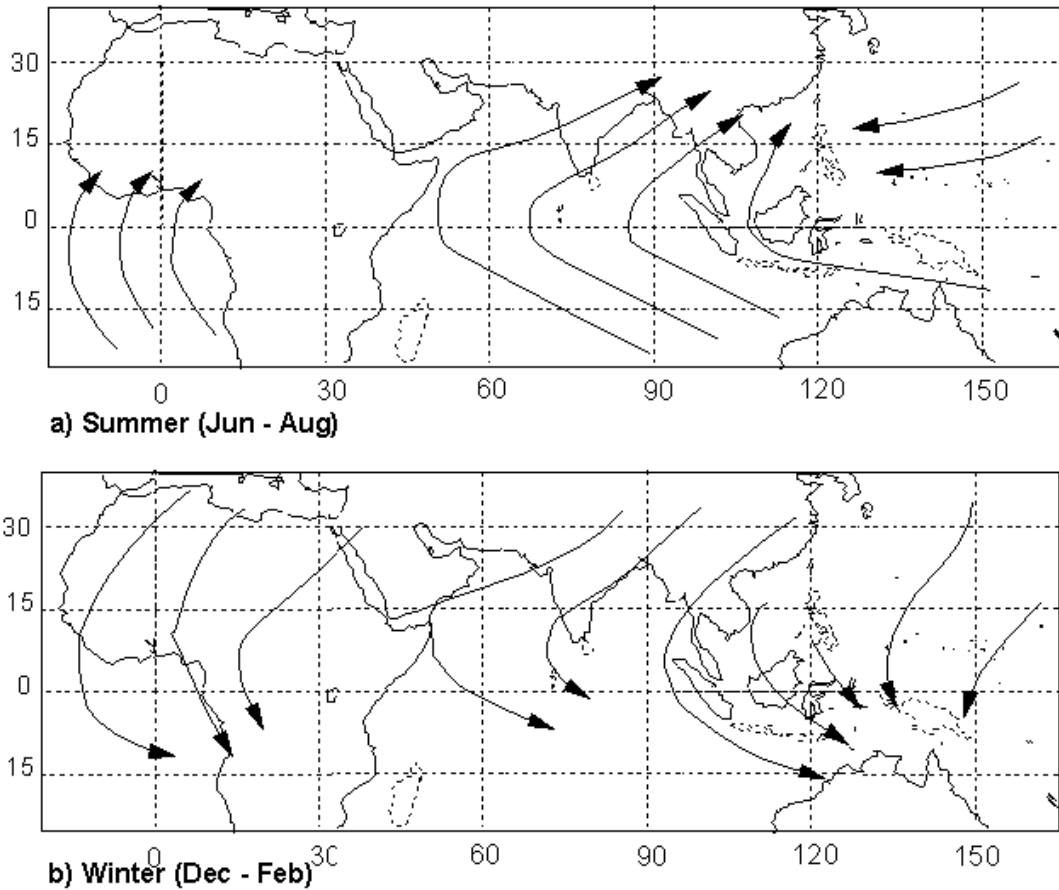


Figure 1.6 Surface winds in northern hemisphere during (a) summer (b) winter (Webster, 1987)

Once the season has begun, forecasts of daily rainfall are attempted by observing and predicting the lengths of "active" and "break" periods. They are characterized by transient precipitation maxima and minima over south Asia or northern Australia, depending on the season. These periods are thought to be associated with shifts in the location of the monsoon trough. During the monsoon break the monsoon trough moves northward to the foot of the Himalayas, resulting in decreases of rainfall over much of India but enhanced rainfall in the far north and south (Ramanadham et al., 1973). These anomalies are large scale and extend across all of south Asia. Breaks and active periods vary in duration and may last between a few days and weeks, identified

by fluctuations in the typical weather pattern. Das (1987) identified several features associated with the active phase, which brings rain to the northern Indian Plains and its west coast. They include tropical depressions in the Bay of Bengal, a low-level jet stream along the east African coast, and the variations in the monsoon trough, the area of low pressure that develops over India during the summer monsoon season.

Active and break periods of the north Australian summer monsoon appear to have a different signature from those of the northern hemisphere summer. Rather than exhibiting north-south oscillations, the convection appears to propagate zonally (McBride, 1983). However, the space scales and timescales of the events are quite similar (McBride et al. 1995, Fasullo et al., 2000). Hendon et al. (1997) notes that there are large differences in the frequency of active and break periods from year to year in the Australian monsoon.

1.5 Previous research on the precipitation and outflow from the Ganges catchment

The Ganges and Brahmaputra catchments are located over central India and the foothills of the Himalaya, respectively. Whitaker et al. (2001) concentrated on the Ganges river discharge and found a relatively strong relationship between annual river flow and the extremes of ENSO and their time derivatives. These relationships are not surprising given the relatively strong relationship between Indian rainfall and ENSO. The relationship between the tendency of ENSO and Ganges river discharge reflects the observation of drought conditions over India during the summer before the maximum amplitude El Niño and a flood year in the summer following the maximum (Yasunari 1990, Shukla 1983). Whitaker et al. (2001) suggested that the ENSO-Ganges discharge relationship may be a basis for long-term predictive capability. The utility of this idea must be considered in the decadal waxing and waning of the seasonal mean Indian rainfall and ENSO (e.g., Torrence et al. 1998, 1999, 2000, Stephenson et al. 1999). Clark et al. (2000), on the other hand, found that there was increased predictability of Indian precipitation when an index was formed that took into account the SST variability in regions of the tropical Indian Ocean, in addition to ENSO information. Chowdhury (2003) concentrated on the relationships between ENSO and rainfall in Bangladesh which is located at the confluence of the Ganges, Brahmaputra and the Meghna (see Figure 1.1). He found little correspondence between the Southern Oscillation Index (SOI) and local rainfall over Bangladesh. He discovered a stronger relationship between river discharge and the

SOI, probably reflecting the SOI-Indian rainfall relationship discussed above. Chowdhury's results are not particularly relevant to the issue of river discharge in this region as it has been estimated that only 10-15% of the rainfall over Bangladesh itself contributes to the river flow in the delta. More relevant, then, is the variability of rainfall over the much larger catchment areas of the Brahmaputra and the Ganges.

The precipitation in these two regions (and hence the associated river discharge) tend to be out of phase on intraseasonal time scales (Webster et al. 1998, Lawrence et al. 2002, Ferranti et al. 1997). Thus, to a large degree, the river discharge into Bangladesh from the two regions tends to be out of phase: during a break phase in the monsoon it is dry over central India but abundant precipitation falls over the foothills of the Himalayas. During an active phase of the monsoon there is a wet period over central India and a rainfall deficit near the Himalayas. Therefore, to a very large degree, the regional pattern of seasonal flooding in Bangladesh is determined by the waxing and waning of the intraseasonal variability of the Indian monsoon.

Intraseasonal variability is the dominant mode of monsoon variability. Numerical models are still being developed to predict or simulate variability in the 10-40 day time scale (e.g., Schiller, 2003, Keppenne, 2000). However, it has been firmly established that predictability on these time scales does exist. For example, Webster et al. (2004) have been able to show substantial forecasting skill in the 20-30 day range using an empirical Bayesian forecast system. These forecasts have been applied in

experimental operational predictions under the auspices of the Climate Forecast Applications in Bangladesh (CFAB¹). Thus, to a certain degree, the forecast of the intraseasonal variability of river discharge over this region is in hand. However, for long-term planning of water resource management and disaster relief preparation, it is necessary to anticipate the integrated seasonal discharge of the monsoon river.

In this research project a newly available river discharge data set was used to examine the detailed relationships between the discharges of these two great rivers and SST variability over the tropics. The aim is to determine whether or not there are useful signals in the evolving climate system on time scales of a month or longer that would help in the long-term prediction of river flow levels in the Brahmaputra-Ganges River delta. Such information could prove very useful for long-term planning of water resource management and agricultural practices and disaster relief preparation.

¹ The 20-30 day forecasts are part of a three-tier prediction system, Real-time forecasts can be seen at <http://cfab2.eas.gatech.edu>. A full description of the project is given at <http://cfab.eas.gatech/html>

CHAPTER 2

DESCRIPTION OF DATASETS

Monthly discharge data is calculated from daily river discharge observations made at staging stations at Bahadurabad on the Brahmaputra, and at Hardinge Bridge on the Ganges. Both stations lie close to the Bangladesh-Indian border (marked as red circles in Figure 1.1). The daily Ganges and Brahmaputra discharge data used in the study extends from 1950 to 2003 and 1956 to 2003, respectively. Isolated missing data points were replaced by linear interpolation. Longer missing periods (several winters and all of 1971) were replaced by climatology mean values. Data was obtained from the Bangladesh Flood Forecast and Warning Center in Dhakar, Bangladesh. Times series of the river discharge is shown in Figure 2.1.

SST data was retrieved from NOAA Extended reconstructed SST dataset (Smith et al. 2003). It was constructed using the most recently available Comprehensive Ocean-Atmosphere Data Set (COADS) SST data and improved statistical methods that allow for stable reconstruction of sparse data. This monthly analysis begins January 1854 and extends to December 2003 with a resolution of two degrees latitude by two degrees longitude. In this research, only data for the period from 1950 to 2003 are considered to match the discharge data.

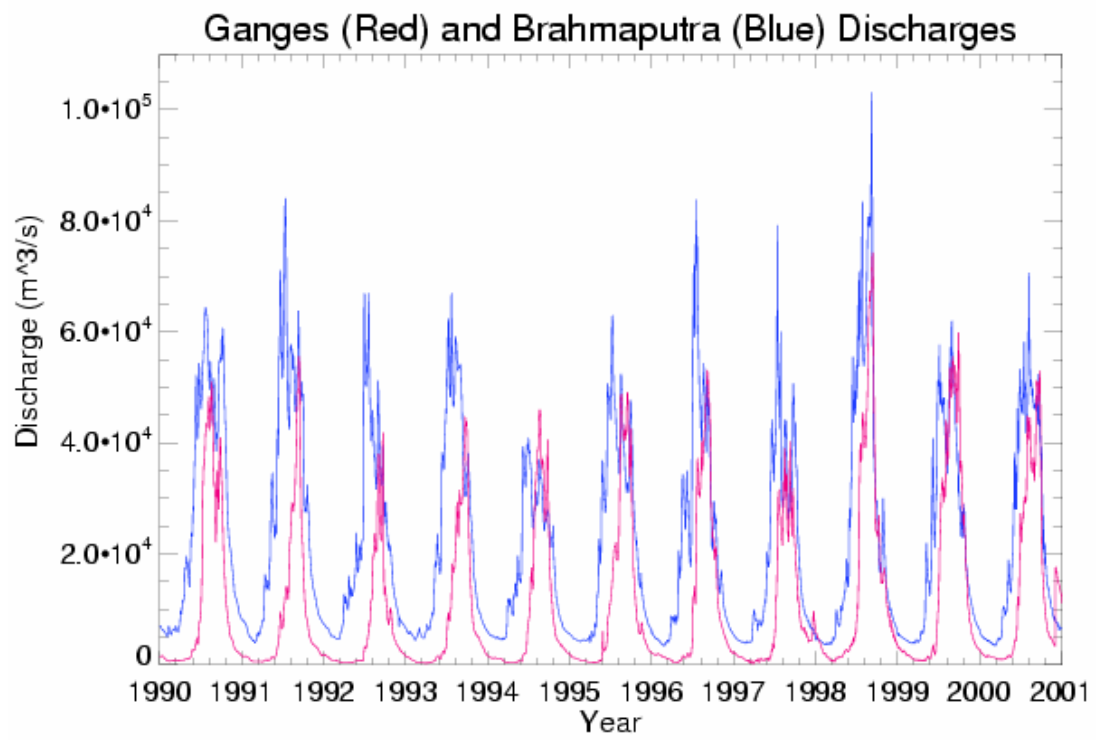


Figure 2.1 Time series of Brahmaputra-Ganges River discharge over period 1990-2000

CHAPTER 3

RESULTS AND DISCUSSIONS

3.1 Relationship between Brahmaputra discharge and SST

3.1.1 Seasonal Relationship

Figure 3.1 shows correlations between the mean seasonal (July to September denoted by JAS) Brahmaputra River discharge into Bangladesh and tropical Indo-Pacific SST at different seasonal lags using all years of available data. Shaded areas denote regions with correlation coefficients greater than 0.2. The 95% confidence level ($r=0.29$) is marked by a solid black line. Panel (a) shows the correlation between JAS discharge and the subsequent October through December (OND) SST, panel (b) denotes simultaneous correlations, panel (c) the JAS discharge and the prior April through June (AMJ) SST, and panel (d) the JAS discharge with the prior January and March (JFM) SST. Overall, Figure 3.1 (a)-(d) show very strong and broad scale correlations especially over the Indian Ocean. Panels (e)-(h) in Figure 3.1 show the same correlations but with the omission of data from the year 1998. The correlations are severely reduced indicating that 1998 contributed a strong bias to the overall correlations. As it turns out, the summer of 1998 was an exceptional year in terms of the magnitude of the north Indian Ocean SST anomaly (e.g. Webster et al. 1999 and Saji et al. 1999) which reached an unprecedented 1.5°C above normal, and occurred at the time of the 1997-1998 El Niño. During this period, widespread floods extended across 60% of Bangladesh for most of the summer period. Over the summer

of 1998, the Brahmaputra River discharge into Bangladesh reached 160% percent of normal. Whereas there is usually a warming of the Indian Ocean associated with the declining phase of an El Niño (Shukla 1983), it is generally much weaker than that which occurred during the summer of 1998.

In summary, with 1998 excluded, the SST-Brahmaputra discharge relationship is reduced to modest regional simultaneous correlations in the Bay of Bengal. Statistically, the 1998 data represents an outlier that provides little contribution to the determination of long-term predictability. We can conclude that Brahmaputra River discharge is not significantly connected to ocean SST variance over long time periods. Whether or not the unique and anomalous state of the Indian Ocean during the 1998 period resulted in the excessive discharge is unclear, requiring experimentation with numerical climate models. Irrespective of the answer, it is clear that 1998 is not representative of the long term predictability of the Brahmaputra River discharge.

3.1.2 June Brahmaputra discharge and northwest Pacific SST

On the other hand, the June Brahmaputra River flow is significantly correlated with SST in northwest Pacific Ocean to the east of Japan (150°E - 180°E , 35°N - 45°N) during the months preceding spring and winter. The maps of correlation contours and scatter plots (between June and antecedent months) are shown in Figure 3.2 and Figure 3.3, respectively. In the scatter plots, the ENSO effect is also examined using Null's (2003) categorization. Triangles denote data collected during an El Niño year and squares show data from La Niña years. Stars show data from years that were neither El Niño nor La Niña. There is not a significant relationship during ENSO events. Considering that most of the May and June Brahmaputra flow results from the melted snow cover pack over the Tibetan Plateau, it is possible that the northwest Pacific SST is related to upstream winter storm activity that causes more Tibetan snowfall. However, this hypothesis has not been tested.

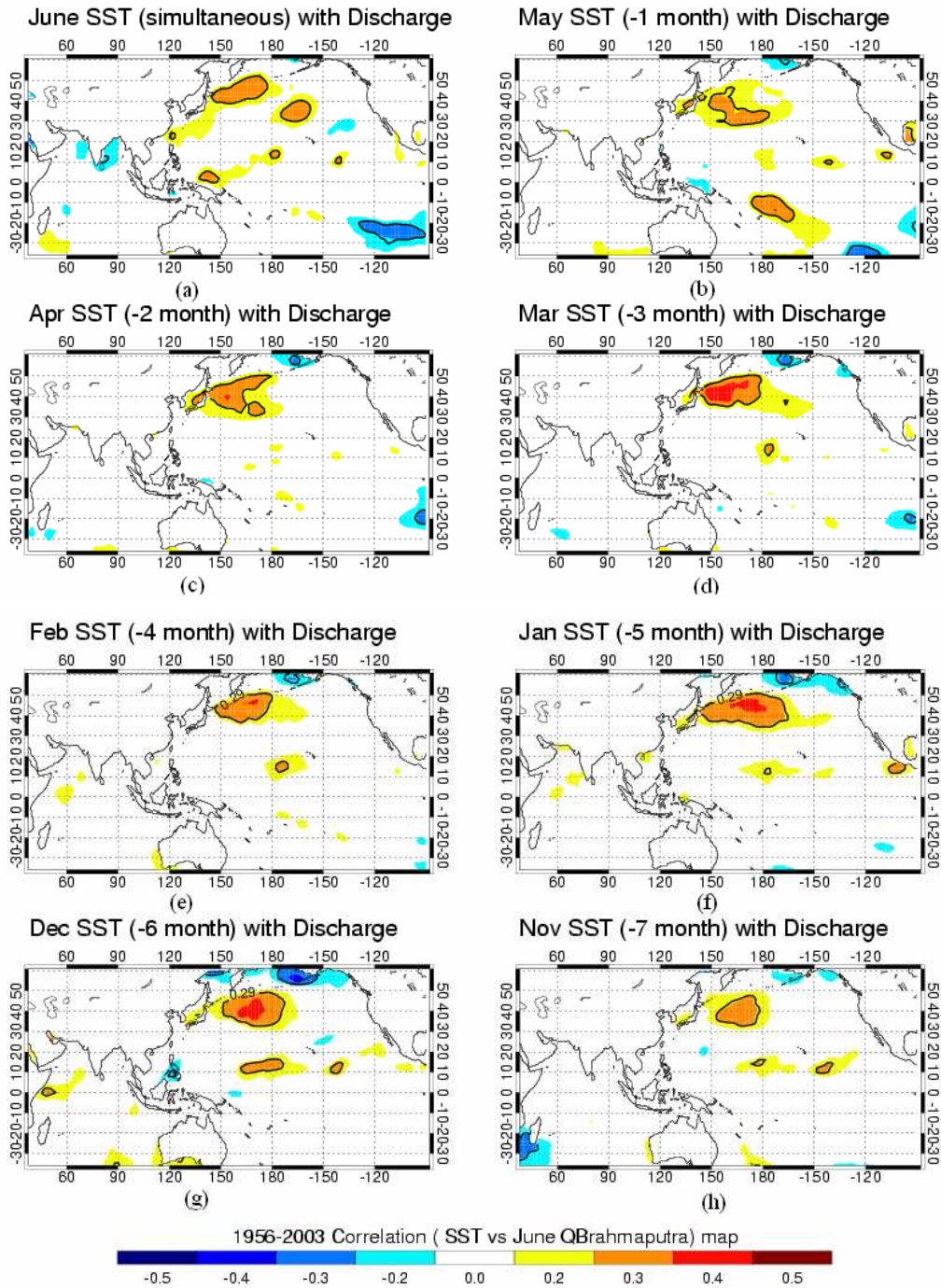


Figure 3.2 Relation map of June Brahmaputra discharge and lead time northwest Pacific SST over period 1956-2003, Panel (a)-(h) show the correlation between discharge and antecedent monthly SSTs from June to November

June Brahmaputra discharge vs northwestern Pacific SST

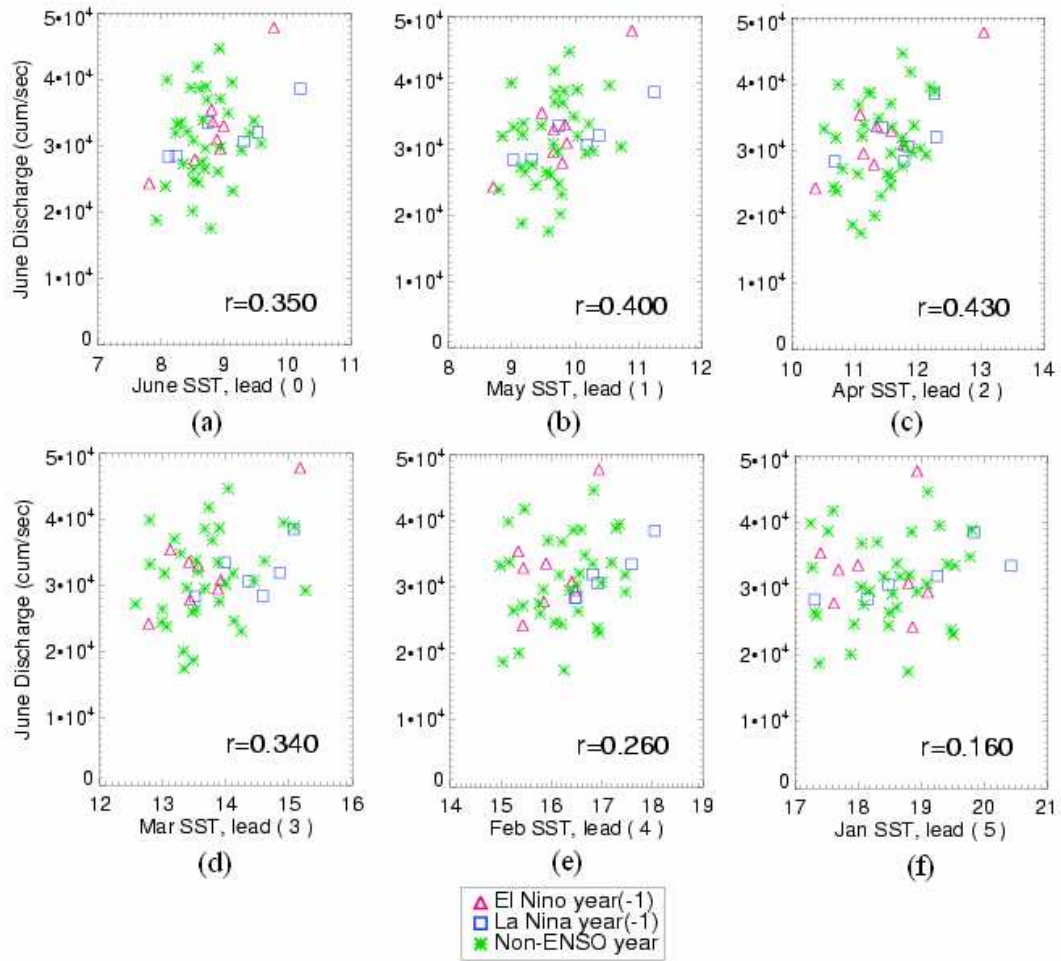


Figure 3.3 Scatter points of June Brahmaputra discharge verses northwest Pacific Ocean SST index. Panel (a)-(f) denote the scatter plots of the two variables, respective to Figure 3.2 (a)-(f), colored symbols denote different ENSO categories. Correlation coefficients are plotted

3.2 Relationship between Ganges discharge and SST

3.2.1 Boreal summer discharge and SST

The relationship between the Ganges discharge and regional SST are very different from those found for the Brahmaputra. Maps of correlations for the same lags are displayed in Figure 3.4(a)-(d). In panels (a), (b) and (c), strong negative correlations (cool colors) occur in the central equatorial Pacific and also eastward and the north of the equator. On the other hand, strong positive correlations (warm colors) occur in the western and southwestern Pacific Ocean. The strong positive correlations over the southwest Pacific Ocean to the east of Australia persist throughout the period. In addition, relatively strong relationships exist with the subtropical northwest Pacific SST. These out-of-phase correlations between the Nino 3.4, the southwest Pacific Ocean and the northwest Pacific Ocean match the SST anomaly patterns associated with the ENSO cycle. Overall, the strong SST-Ganges discharge correlations one season ahead appear to suggest that useful predictability may exist for the Ganges discharge.

It is interesting to note that there is a relative absence of correlations between SST in the Indian Ocean and Ganges discharge. Also, unlike the Brahmaputra case, the inclusion of 1998 makes little difference to the correlations shown in Figure 3.4. The absence of a link with the regional SST seems strange because the Indian Ocean plays an integral part in the dynamics of the monsoon circulation through heat and

moisture transfer (e.g., Webster et al. 1998). Also, the result is not in keeping with the moderate relationships between Indian Ocean SST and All-India rainfall found by Harzallah and Sadourny (1997) and Clark et al. (2000). Given that river discharge is essentially the integral of rainfall over a catchment's area, one would expect stronger correlations with regional SST variability than that displayed in Figure 3.4.

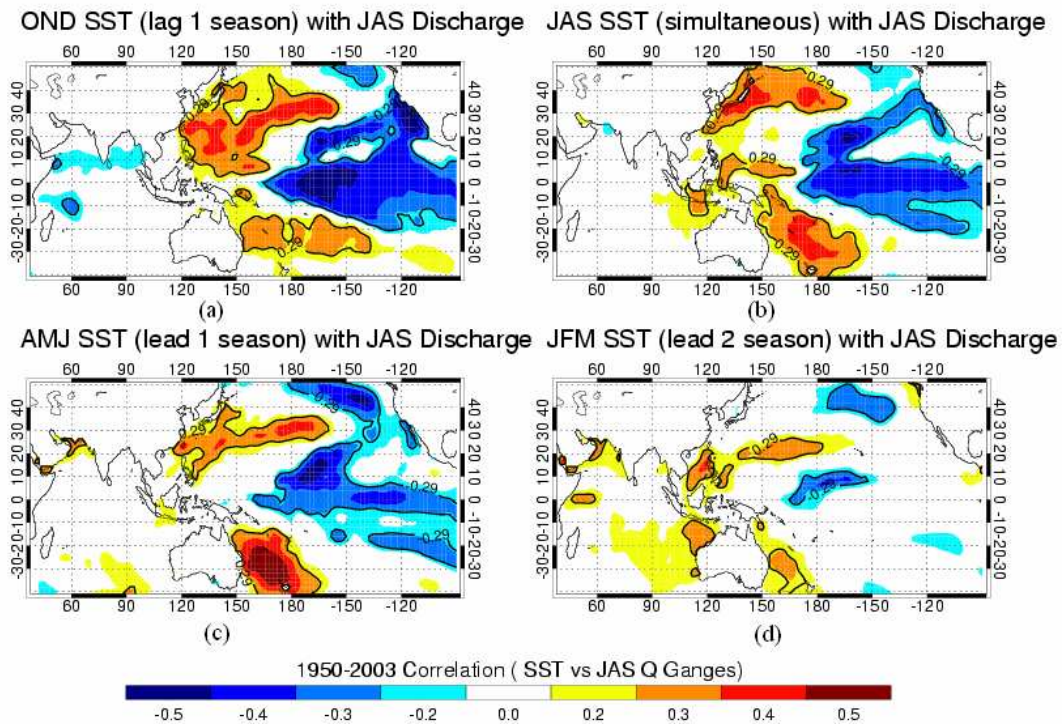


Figure 3.4 Correlation map of Seasonal (Jul-Aug-Sep) Ganges discharge with (a) one season lag (Oct-Nov-Dec) SST (b) simultaneous SST (c) one season lead (Apr-May-Jun) SST (d) two season lead (JFM) SST; solid black contour denotes the 0.95 significance level

3.2.2 Monthly discharge with monthly SSTs

The analysis is extended by correlating monthly Ganges discharge with monthly SST at different lags. In Figure 3.5 the July Ganges River discharge is correlated with the July, June, May and April SSTs (panel a-d) while the August discharge is correlated with the August, July, June and May SSTs (panel e-h). All correlation patterns are similar to those found in the seasonal calculations. The high negative (positive) correlation regions in the central equatorial (southwest) Pacific continue exist for lags -2 months to lag 0. Similarly, the moderate northwest Pacific correlations also persist. The highest correlation value observed is greater than 0.6 and occurs in the southwest Pacific Ocean between the May SST and July Ganges flow, meaning that more than 36% of the July Ganges River discharge variability can be explained by the southwest Pacific SST two month ago.

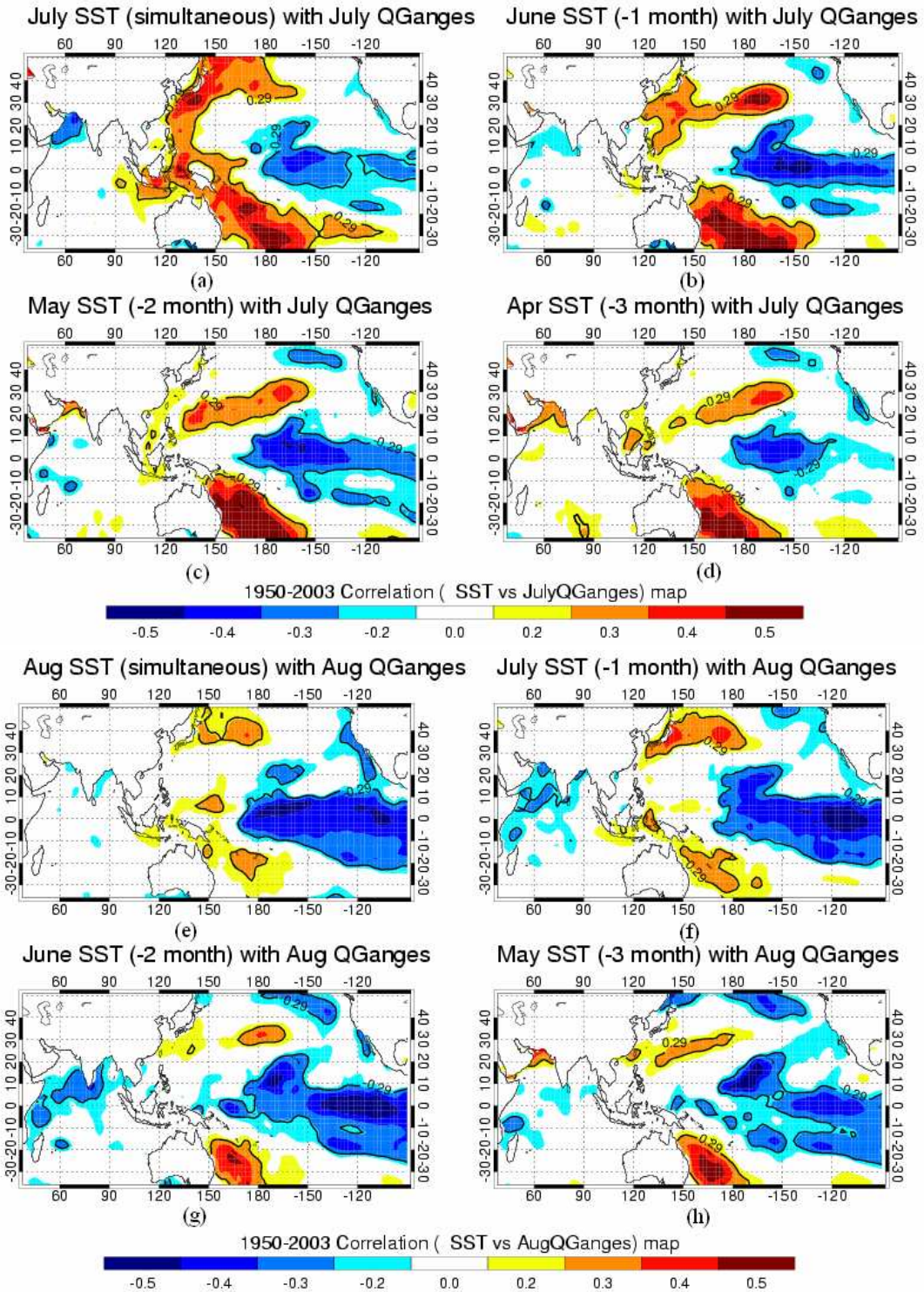


Figure 3.5 Correlation map of July Ganges discharge with (a) July SST (b) June SST (c) May SST (d) Apr SST; August Ganges discharge with (e) August SST (f) July SST (g) June SST (h) May SST

Figure 3.6 presents a systematic display of the lead-lag correlations between river discharge for the two rivers and the areas of significant correlation found in Figure 3.4 and 3.5. Figure 3.6 (a-b) shows the seasonal relationships between SST in Nino3.4 and a particular region in southwest Pacific Ocean (160°E-180°E, 30°S-20°S) over a three year period. Figure 3.6(c-d) shows the July and August discharge lag correlations with Nino 3.4 while Figure 3.6(e-f) shows the same for the southwest Pacific Ocean. Y(0) denotes the years during which the river flow is measured while Y(-1) and Y(+1) refer to the preceding and following years. The dashed lines denote the 95% confidence limits. For all lags and in all regions considered, the Brahmaputra discharge and SST relationships do not exceed the confidence levels. The Ganges, on the other hand, is significant in both regions and months considered. For example, the JAS Ganges discharge is significantly correlated with the Nino 3.4 SST from March of Y(0) through March of Y(+1) (Figure 3.6a). This is similar to the lag relationships found by Yasunari (1990) between Nino 3 SST and All India rainfall. Similar lag-lead relationships are found between the Ganges river discharge and the southwest Pacific Ocean SST. The major difference between the two regions is the shape of the correlation curves. The Nino 3.4 correlations tend to slowly increase with time through year Y(0) whereas the southwest Pacific Ocean correlations change rapidly during the early spring of Y(0). Similar lags and leads are found in the monthly correlations (Figures 3.6c-f).

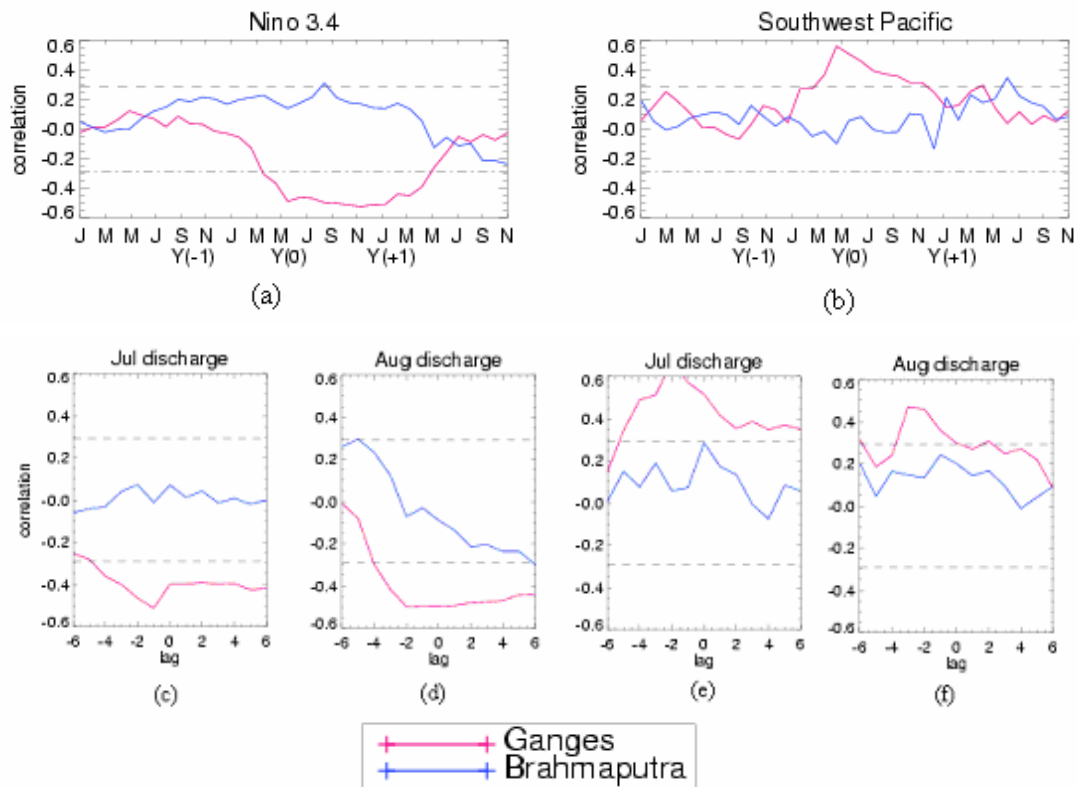


Figure 3.6 Lagged correlations between two river discharges of (a) JAS seasonal average with Nino 3.4 SST (b) JAS seasonal average with southwest Pacific SST (c) July with Nino 3.4 SST (d) August with Nino 3.4 SST (e) July with southwest Pacific SST (f) August with southwest Pacific SST

3.3 Verification results by other analysis methods

3.3.1 Outliers detection by scatter plots

To demonstrate that the relationships between Pacific SST and Ganges river discharge are not the result of individual large anomaly events occurring during one year, such as found for the Brahmaputra in 1998, scatter plots of July Ganges discharge and the SST in the two regions are shown in Figure 3.7. Least square linear regression line and correlation coefficient are shown in the diagram accordingly. The symbols represent for the same ENSO categorization as in Figure 3.3. El Niño years usually accompany low Ganges discharge whereas La Niña years are associated with high Ganges discharge. However, extreme discharge years are also observed to occur when there is no corresponding ENSO extreme. It suggests that the relationship between May southwest Pacific SST and July Ganges flow is much linear and substantially influenced by ENSO episodes even though the relation itself may not be introduced by ENSO events.

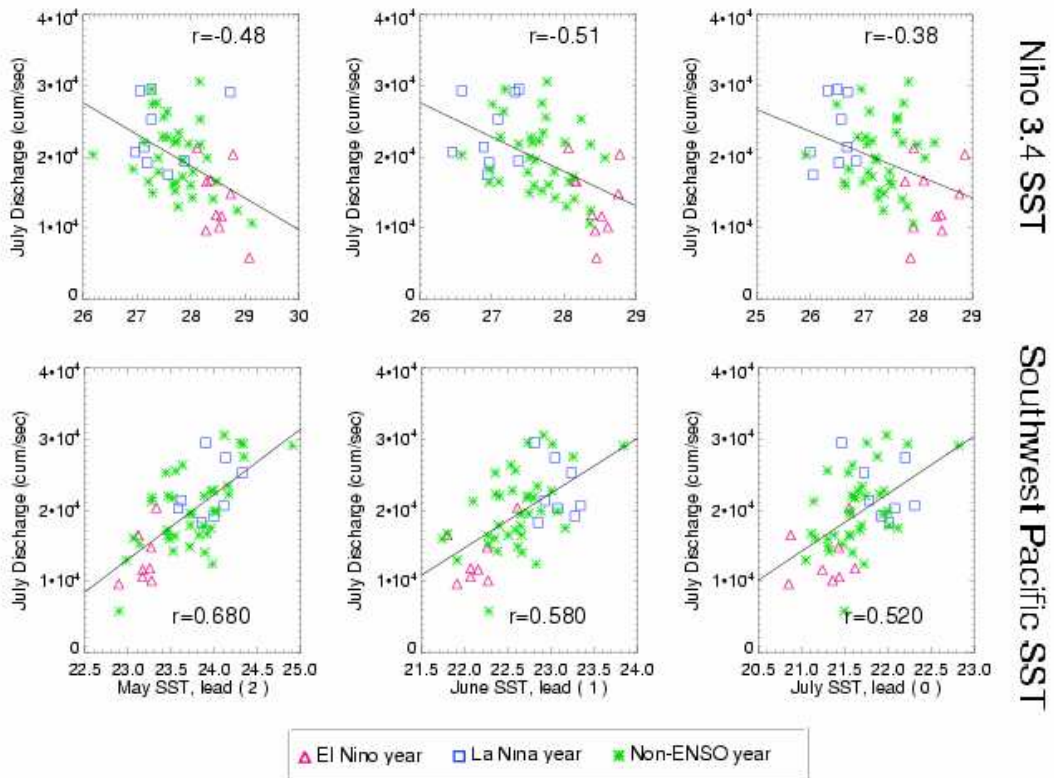


Figure 3.7 Scatter points of SST regions versus July Ganges discharge data with linear regression line. The correlation coefficient and fitted linear regression line are shown on each figure.

3.3.2 Significance study by composite analysis

Figure 3.8 shows composites of the daily boreal summer discharge for both rivers binned according to the extremes of ENSO using the Null's categorization over a 50 year period. The black solid line represents the mean daily discharge of each river. Red/blue/green solid lines denote the composite of daily discharge during El Niño / La Niña / Non-ENSO cases. The composites are plotted relative to the peak Nino 3.4 SST anomaly shown in the upper part of the two panels. Thus Y(-1) refers here to the year preceding the January extreme in SST anomaly and Y(+1) refers to the year following the January extreme. The black dash lines denote the 95% confidence interval deduced using Monte Carlo methods. The Nino 3.4 SST anomaly is also shown in the upper part according to ENSO catalogue as a reference.

The composite Ganges discharge for the La Niña case rises above the 95% confidence level from mid-July to September and continues at this high level through Y(-1). The El Niño composite of discharge is below average attaining statistical significance during August of Y(-1). The Ganges discharge returns to climatological values after August Y(-1). In year Y(+1), the La Niña case shows below average discharge but not at levels exceeding the 95% confidence mark. During the year following an El Niño (Y(+1)), the discharge appears to be normal. The Brahmaputra River did not show anomalous discharge during either El Niño or La Niña.

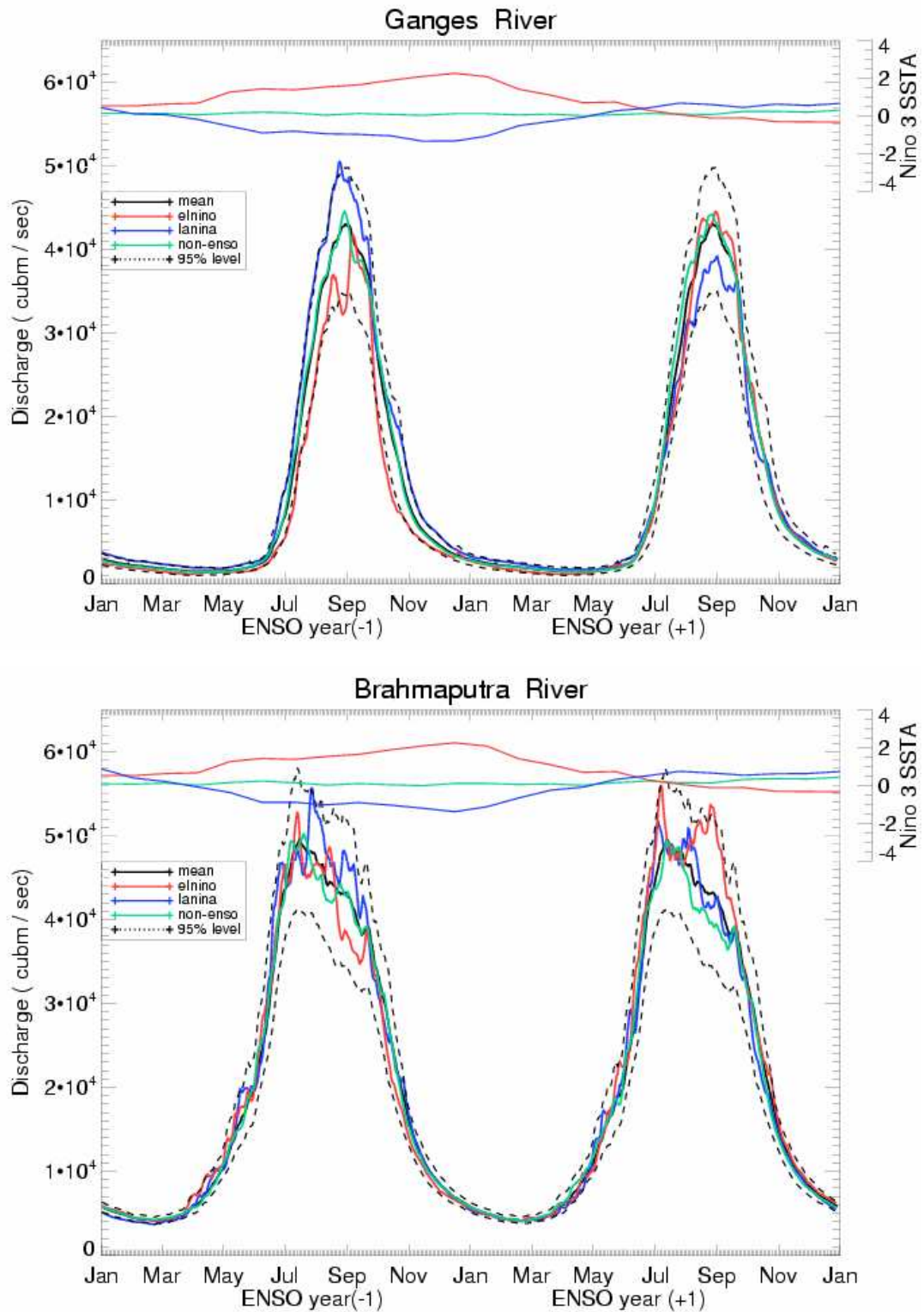


Figure 3.8 Composite analysis of Ganges and Brahmaputra discharge relative to ENSO. The Nino 3.4 SSTA is shown in the upper part according to ENSO catalogue.

3.3.3 Summer river discharge in different ENSO periods

From the above discussions we know that the Ganges discharge is strongly related to ENSO events but Brahmaputra is not. There are only 11 El Niño and 11 La Niña years during the period of 1950-2003 based on Null's categorization. Considering that the frequency of drought or flood disasters in Bangladesh is every three to five years, it would be very useful to compare the probability of excessive discharge during ENSO episodes. In Figure 3.9 each river's summer flow is calculated from June to September (denote JJAS). June discharge is added in addition to the JAS seasonal data in order to contain more information. In Figure 3.8 we know that magnitude difference in monthly discharge between the winter and summer time is more than ten times. In Ganges River case, the major discharge is concentrated in July, August and September. But for Brahmaputra River, the discharge begins to develop from June. For more accuracy, the June discharge should be counted even it is few for Ganges.

The total numbers of recorded years (50 for Ganges River and 44 for Brahmaputra River) are stratified according to ENSO category and the magnitude of river discharge (mean and mean \pm standard deviation). The scheme shows that the Ganges River flow exhibits considerable sensitivity to ENSO years, i.e. strong likelihood of flooding during La Niña years and droughts during El Niño years. Both the moderate category (within mean \pm standard deviation) and extreme category (beyond mean \pm standard deviation level) suggest this. The Brahmaputra River is less sensitive to ENSO events. Flood conditions may happen in either situations - El Niño

or La Niña. The Brahmaputra schematic also suggests that drought conditions are more likely during El Niño years. On the other hand, in either case (Ganges or Brahmaputra) there is substantial fraction of drought/flood events during Non-ENSO years.

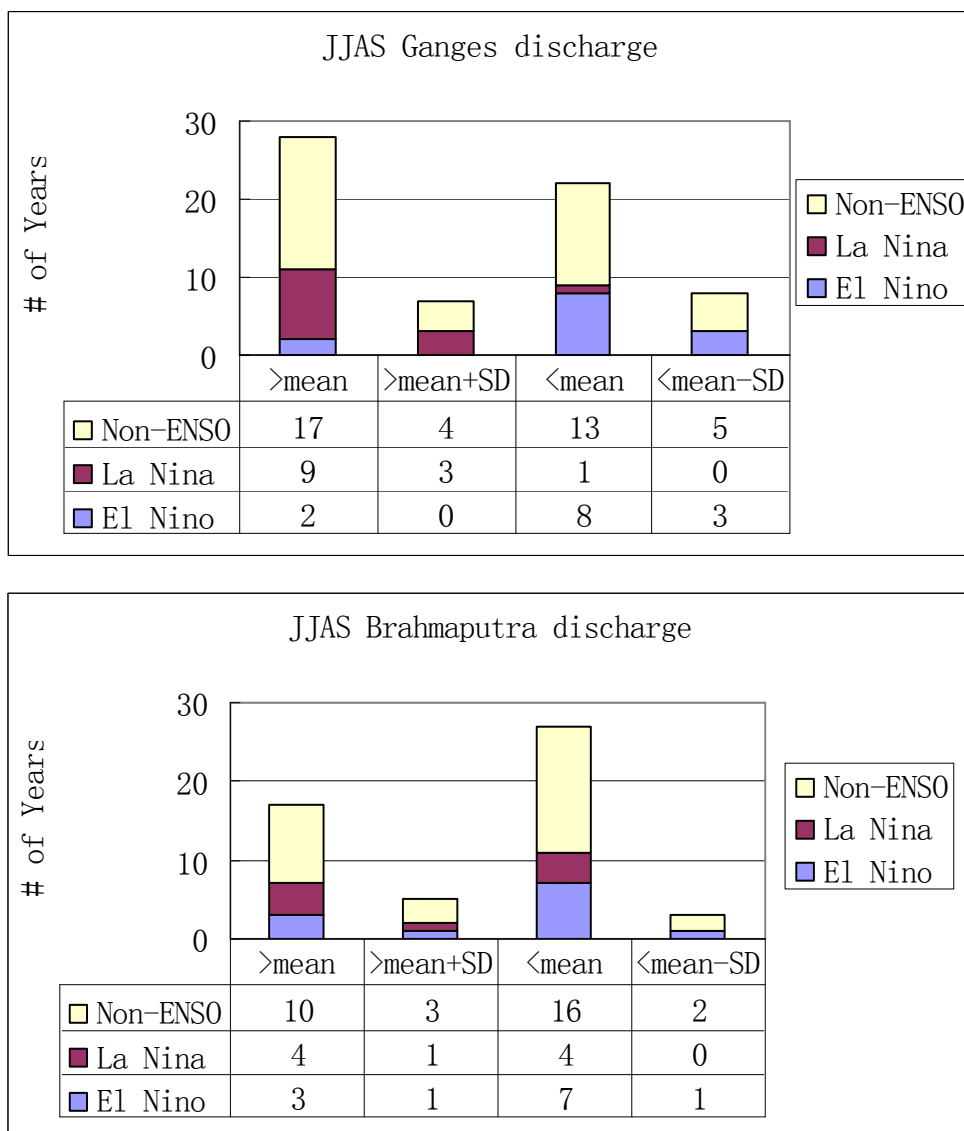


Figure 3.9 JJAS discharge categorized by ENSO and magnitude (the columns denote the categories of discharge level: above average, above mean plus one standard deviation, below average, and below mean minus one standard deviation; colors depict the different ENSO episodes)

3.4 The SST evolution relative to southwest Pacific SST

The preliminary attempts to explore the influential mechanism between the southwest Pacific SST and summer Ganges discharges starts from the precursors. Once again the correlation analysis technique is used to make contour maps. The question is how does the lead-lag time SSTs in the Indian Ocean and the Pacific Ocean vary with the southwest Pacific SST variation. In the lead-time scale (Figure 3.10), the May southwest Pacific SST and the SSTs from simultaneous to the prior three months in the same calendar year are depicted. It appears that only the April southwest Pacific SST has a statistical significant association. In the lag-time scale (Figure 3.11), the May southwest Pacific SST has a much stronger correlation with the subsequent SST. Moreover, the main responded SST area moves from May time southwest Pacific Ocean to eastern equatorial Indian Ocean in July and August; the period during which the Intertropical Convergence Zone (ITCZ) is active in Bay of Bengal. Therefore, the effect of the SST to the onset and evolution of South Asian summer monsoon is suggested. It has been pointed out by Flatau et al (2001, 2003) that the SST evolution in the Bay of Bengal and the western Pacific plays an important role during the development of summer monsoon. By using a numerical model, she found that a monsoon like perturbation in mid-May followed by a heat wave in India actually delayed the onset of the monsoon.

SST variability in certain areas bears a good correlation with May southwest Pacific SST within all the periods studied, such as the eastern equatorial Indian Ocean (positive) and Nino3.4 region (negative). The values of coefficient are modest but still beyond the 0.90 significant levels. It indicates that the southwest Pacific SST variations are well connected with both eastern equatorial Indian Ocean and mid-equatorial Pacific SST variations. The former plays an important role during the monsoon heat and moisture transporting process and has a great influence on ITCZ; the latter is the main representative of ENSO event. The research results of the interaction between ENSO event and monsoon are mixed. Though it is observed that ENSO may be important in influencing monsoon rainfall variability, there are a large number of factors that may confound or limit monsoon predictability (Lau 2003). I wish my research could provide some useful information in this field.

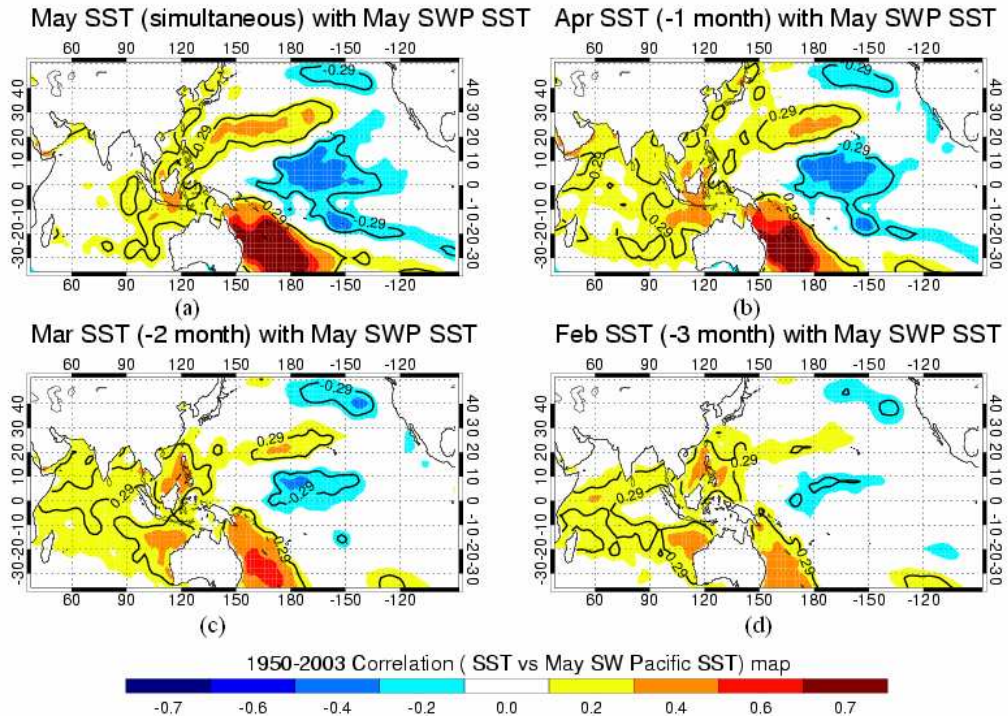


Figure 3.10 Correlation map of May southwest Pacific SST with (a) May SST (b) April SST (c) March SST (d) February SST

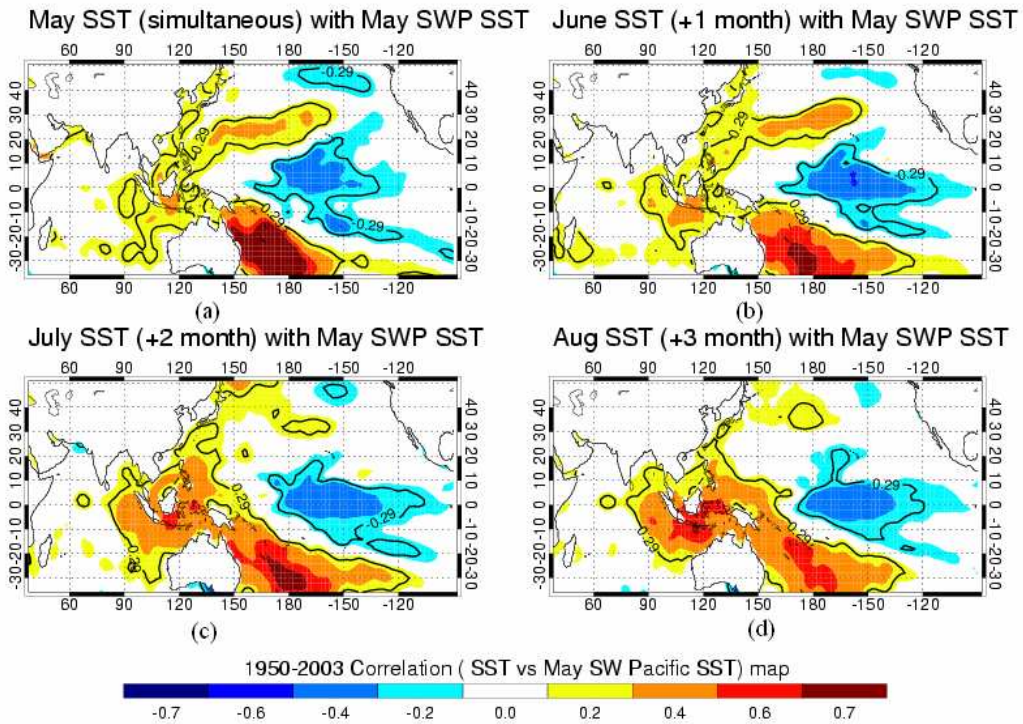


Figure 3.11 Correlation map of May southwest Pacific SST index with (a) May SST (b) June SST (c) July SST (d) August SST

CHAPTER 4

CONCLUSIONS AND FUTURE EXPECTATIONS

Correlation and composite analyses show that there is a significant negative linear relationship between equatorial/southwest Pacific SST and Ganges River discharge from zero to three month lead time consistent with the influence of ENSO on Indian precipitation. Also, the May SST of the southwest Pacific SST to the east of Australia shows a high positive correlation (>0.6) with early summer Ganges discharge. These results indicate that there may be a prospect to statistically predict Ganges flow with a monthly scale time. These results confirm the optimism for forecasting expressed by Whitaker et al. (2001). High latitude SST to the east coast of Japan bears a statistical influence to the June Brahmaputra discharge possibly due to the SST forcing on the genesis of winter storm in East Asia.

The theoretical explanation for this relationship between SST and discharge is still in progress. Regional atmosphere-land-ocean coupled simulations could be expected after proper hypothesis is brought out. The applicable statistical forecasting of the Ganges boreal summer discharge or the onset of the Indian summer monsoon would benefit both the general people in Bangladesh delta and the scholars in this field. It will also be good to know if the northwest Pacific SST contributes to the winter storm genesis. The significance of the June Brahmaputra flow may be better understood by studying the interannual variability of snow characteristics and their relationship to the Himalaya downside flow and SST variations.

REFERENCES

- Amarasekera, K.N., R.F. Lee, E.R. Williams, and E.A.B. Eltahir, 1997, ENSO and the natural variability in the flow of tropical rivers, *J. Hydrology*, 200 (1-4), 24-39.
- Chowdhury, M.R., 2003, The El Niño-Southern Oscillation (ENSO) and seasonal flooding – Bangladesh, *Theor. Appl. Climatol.*, 76,105-124.
- Clark, C. O., J. E. Cole, and P. J. Webster, 2000, SST and Indian summer rainfall: predictive relationships and their decadal variability. *J. Climate.*, 13, 14, 2503-2519.
- COMET-IT (Commonwealth Network of Information Technology for Development), Disasters in Bangladesh, Retrieved September 12, 2004 from <http://www.comnet.mt/bangladesh/distrFlds.htm#Flds>
- Das, P. J., 1987, Short and Long range Monsoon Prediction in India, *Monsoons*, Chapter 17, Eds. Fein & Stevens, Wiley, New York.
- Eldaw, A.K., J.D. Salas, and L.A. Garcia, 2003, Long-Range Forecasting of the Nile River Flows Using Climatic Forcing, *J. Appl. Meteor.*, 42, 890-904.
- Ericksen N.J., Ahmad Q.K. & Chowdhury A.R., 1997, Socio-Economic Implications of Climate Change for Bangladesh, Bangladesh Unnayan Parishad (BUP), Dhaka, Bangladesh, Briefing Document, No. 4, Pp 4.
- Fasullo, J. T. and P. J. Webster, 2000, Atmospheric and surface variations during westerly wind bursts in the Tropical western Pacific, *Q. J. Roy. Met. Soc.*, 126, 899-924
- Ferranti L., J.M. Slingo, and T.N. Palmer, Hoskins B.J., 1997, Relations between interannual and intraseasonal monsoon variability as diagnosed from AMIP integrations, *Quart. J. Roy. Meteor. Soc.*, 123, 541, 1323-1357.
- Flatau, M. K., P.J. Flatau, D. Rudnick, 2001, the Dynamics of Double Monsoon Onsets. *Journal of Climate*, 14, 21, 4130–4146.
- Flatau, M. K., P. J., Flatau, J. Schmidt, and G. N. Kiladis, 2003, Delayed onset of the 2002 Indian monsoon, *Geophys. Res. Lett.*, 30, 14, 1768-1771.
- Harzallah, A. and R. Sadourny, 1997, Observed lead-lag relationships between Indian

- summer monsoon and some meteorological variables, *Climate Dyn.*, 13, 9, 635-648.
- Hendon, H., and C. Zhang, 1997, Propagating and standing components of the Intraseasonal Oscillation in tropical convection, *J. Atmos. Sci.*, 54, 741--752.
- Joint Agricultural Weather Facility, US Department of Agriculture/NOAA, Appendix III, Major World Crop Areas and Climatic Profiles, *Agriculture Handbook No.664* Retrieved September 12, 2004 from
<http://www.usda.gov/oce/waob/jawf/profiles/specials/monsoon/monsoon.htm>
- Keppenne, C.L., S.L. Marcus, M. Kimoto, and M. Ghil, 2000, Intraseasonal Variability in a Two-Layer Model and Observations, *J. Atmos. Sci.*, 57, 8, 1010–1028.
- Lawrence, D, and P. J. Webster, 2002, The Boreal Summer Intraseasonal Oscillation: Relationship between Northward and Eastward Movement of Convection. *J. Atmos. Sci.*, 59, 9, 1593-1606.
- Lau, K.M., 2003, Monsoon/ ENSO-Monsoon Interaction, *Encyclopedia of Atmospheric Sciences*, eds Holton, J., Pyle, J., Curry, J., 1386-1391.
- McBride, J. L., 1983, Satellite observations of the southern hemisphere monsoon during Winter MONEX. *Tellus Series A-Dynamic Meteorology and Oceanography*, 35 (3): 189-197, 35A, 189-197.
- McBride, J. L., N. E. Davidson, K. Puri, and G. C. Tyrell, 1995, The flow during TOGA COARE as diagnosed by the BMRC tropical analysis and prediction scheme, *Mon. Weather Rev.*, 123, 3, 717-736.
- Nicholls, N., 2003, El Niño and the Southern Oscillation: in *Encyclopedia of Atmospheric Sciences*, eds Holton, J., Pyle, J., Curry, J., 713-723.
- NCEP (National Center for Environmental Predictions)/CPC (Climate Prediction Center, Washington DC, Retrieved November 10, 2004 from
http://www.cpc.ncep.noaa.gov/products/analysis_monitoring/impacts/warm_impacts.html
http://www.cpc.ncep.noaa.gov/products/analysis_monitoring/lanina/cold_impacts.html
- NOAA a, (National Oceanic and Atmospheric Association), 2004, ENSO background and Description, Retrieved October 10, 2004 from
<http://www.cdc.noaa.gov/ENSO/enso.description.html>
- NOAA b, (National Oceanic and Atmospheric Association), 2004, El Nino Theme Page, Retrieved October 10, 2004 from
<http://www.pmel.noaa.gov/tao/elnino/el-nino-story.html>

- NOAA c, (National Oceanic and Atmospheric Association), 2004, El Nino Theme Page, Retrieved October 10, 2004 from <http://www.pmel.noaa.gov/tao/elnino/nino-home.html>
- Null, J., 2004, El Niño years & La Niña years: A consensus list, CCM, Retrieved October 10, 2004 from <http://ggweather.com/enso/years.htm>.
- Oliver and Fairbridge, 1987, the *Encyclopedia of Climatology*
- Ramanadham, R., P. V. Rao and J. K. Patnaik, 1973, Break in the Indian summer monsoon, *Pure Appl. Geophys.*, 104, 635--647.
- Saji, N.H., B.N. Goswami, P.N. Vinayachandran, and T. Yamagata, Sep 1999, A dipole mode in the tropical Indian Ocean, *Nature*, 401, 6751, 360-363.
- Schiller, A., and J.S. Godfrey, 2003, Indian Ocean Intraseasonal Variability in an Ocean General Circulation Model, *J. Climate*, 16, 1, 21–39.
- SDNP (Sustainable Development Network Programme), 2004, Inter Basin Water Transfer link Project, Retrieved October 10, 2004 from http://www.sdnbd.org/river_basin/bangladesh/bangladesh_water_resources.htm
- Shukla, J. and D.A. Paolina, 1983, The southern oscillation and long range forecasting of the summer monsoon rainfall over India, *Mon. Weather Rev.*, 111, 1830-1837.
- Smith, T.M., and R.W. Reynolds, 2003, Extended Reconstruction of Global Sea Surface Temperatures Based on COADS Data (1854-1997). *J. Climate*, 16, 10, 1495-1510.
- Stephenson, D. B., K. R. Kumar, F. J. Doblas-Reyes, J.-F. Royer, F. Chauvin and S. Pezzulli, 1999, Extreme Daily Rainfall Events and Their Impact on Ensemble Forecasts of the Indian Monsoon, *Monthly Weather Review*: 127, 9, 1954–1966.
- Tawfik, M., 2003, Linearity versus non-linearity in forecasting Nile River flows, *Advances in Engineering Software*, 34, 8, 515-524.
- Torrence, C. and P. J. Webster, 1998, The Annual Cycle of Persistence in the El Niño-Southern Oscillation, *Quart. J. Roy. Meteor. Soc.*, 124, 1985-2004.
- Torrence, C., and P. J. Webster, 1999, Interdecadal changes in the ENSO-Monsoon System, *J. Climate.*, 12, 8, 2679-2690.

- Torrence, C. and P. J. Webster, 2000, Comment on "The connection between the Boreal Spring Southern Oscillation Persistence Barrier and Biennial Variability," *J. Climate*, 13, 3, 665-667.
- Walker, G. T., Correlation in seasonal variations of weather, 1923, VIII, A preliminary study of world weather, *Mem. Indian Meteorol. Dept.*, 24, 75-131.
- Walker, G. T., Correlation in seasonal variations of weather, 1924, IV, A further study of world weather, *Mem. Indian Meteorol. Dept.*, 24, 275-332.
- Walker, G. T., World weather, 1928, III, *Mem R. Meteorol. Soc.*, 2, 97-106.
- Wang, G., and E.A.B. Eltahir, 1999, Use of ENSO information in medium- and long-range forecasting of the Nile floods, *J. Climate*, 12, 6, 1726-737.
- Webster, P.J., 1987, the Elementary Monsoon, *Monsoons*, Eds., Fein & Stevens, Wiley, New York, Ch 1.
- Webster, P.J., V.O. Magana , T.N. Palmer, J. Shukla, R.A. Tomas, M. Yanai, and T. Yasunari, 1998, Monsoons: Processes, Predictability, and the Prospects for Prediction, *J. Geophys Res.*, 103 c7, 14451-14510.
- Webster, P.J., A. Moore, J.P. Loschnigg, and R.R. Leber, Sep 1999, Coupled ocean-atmosphere dynamics in the Indian Ocean during 1997-98. *Nature*, 401, 23, 356-360.
- Webster, P.J., and J. Fasullo, 2003, Monsoon/ Dynamical Theory, *Encyclopedia of Atmospheric Sciences*, eds Holton, J., Pyle, J., Curry, J., 1370-1386.
- Webster, P. J., and C. Hoyos, 2004, Prediction of Monsoon Rainfall and River Discharge on 15-30 day Time Scales, *Bull. Amer. Met. Soc.*, 85, 11, 1745-1765.
- Whitaker, D.W., S.A. Wasimi, and S. Islam, 2001, The El Niño-Southern Oscillation and long-range forecasting of flows in the Ganges, *Int. J. Climatol*, 21, 77-87.
- Yasunari, T., 1990, Impact of Indian monsoon on the coupled atmosphere/ocean system in the tropical Pacific, *Meteorol. and Atmos. Phys.*, 44, 29-41.